

## meson photoproduction at low energies

Yongseok Oh<sup>1,2</sup>, and T.-S. H. Lee<sup>2,y</sup><sup>1</sup>Institute of Physics and Applied Physics,  
Yonsei University, Seoul 120-749, Korea<sup>2</sup>Physics Division, Argonne National Laboratory, Argonne, Illinois 60439

(Dated: May 1, 2020)

## Abstract

The exchange model for photoproduction is re-examined and a new model has been developed by considering the explicit two-pion exchange mechanisms and the  $f_2$  meson exchange. The  $f_2$  exchange is calculated from an effective Lagrangian which is constructed from using the tensor structure of the  $f_2$  meson. Phenomenological information together with tensor meson dominance and vector meson dominance assumptions are used to estimate the  $f_2$  coupling constants. For  $2\pi$  exchange, the loop terms including intermediate  $N$  and  $\Delta$  channels are calculated using the coupling constants determined from the study of pion photoproduction and the use of vector meson dominance assumption. It is found that our model with  $f_2$  and  $2\pi$  exchanges is comparable to the commonly used exchange model in describing the existing differential cross section data. Their differences can be distinguished by examining the single and double spin asymmetries. Predictions are given for future experimental investigations.

PACS numbers: 13.60.Le, 13.60.-r, 13.88.+e, 25.20.Lj

---

Electronic address: yoh@physa.yonsei.ac.kr<sup>y</sup>Electronic address: lee@phy.anl.gov

## I. INTRODUCTION

The recent experiments at Thomas Jefferson National Accelerator Facility (JLAB) [1{4], GRAAL of Grenoble [5], and LEP-S of SP ring-8 [6] are expected to provide new opportunities for studying the electromagnetic production of vector mesons at low energies. For example, the differential cross section data for photoproduction from the CLAS Collaboration at JLAB show big differences with the old data of 1970's [7] in the large momentum transfer ( $\vec{t}$ ) region where one may learn about the  $VNN$  couplings and other production mechanisms [8{11]. Much more new data with similar high precisions will soon be available.

The study of vector meson photoproduction is expected to shed light on the resolution of the so-called 'missing resonance' problem [12{16]. On the other hand, it is well known that this can be achieved only when the nonresonant mechanisms are well understood [17, 18]. As a continuation of our effort in this direction [13, 17], we explore in this work the nonresonant mechanisms of photoproduction.

There exist some investigations of the nonresonant mechanisms for vector meson photoproduction. To account for the radiative features of the data in small  $t$  at high energies, the Pomerion exchange model, as illustrated in Fig. 1(a), was developed. However, this model fails to describe the experimental observables at low energies. Indeed, meson exchanges (or secondary Reggeon exchanges) are found to be crucial in understanding the low energy data. In the case of  $\pi^+$  photoproduction, it is well known that one-pion exchange is the most dominant process at low energies. For photoproduction, however, the situation is not clear. Generally, there are two scenarios which are based on either the meson exchange model [19, 20] or the  $f_2$  meson exchange model [9, 21]. The exchange model was motivated [19] by the observation that the decay width of  $\pi^+$  is much larger than the other radiative decays of the  $\pi$ . It is further assumed that the  $\pi^+$  in the  $\pi^+ N$  channel can be modeled as a meson such that the vertex can be defined for calculating the exchange mechanism as illustrated in Fig. 1(b). In practice, the product of the coupling constants  $g \cdot g_{NN}$  of this tree-diagram is adjusted to fit the cross section data of photoproduction at low energies. If we use  $g_{NN}^2 = 4 \cdot 8$  from Bonn potential, we then find that the resulting  $g$  will yield a decay width of  $\pi^+ \pi^+$  an order of magnitude larger than the value extracted from the experimental decay width of  $\pi^+ \pi^+$  [22, 23]. Furthermore, there is still no concrete evidence on the particle identification of the  $\pi$ , and the use of exchange in  $NN$  potential has been seriously questioned. Thus the commonly used exchange model for photoproduction must be further examined theoretically.

In this work, we take a different approach to account for the exchange of  $\pi^+$  in photoproduction. Instead of considering the radiative decay of the  $\pi^+$  through the  $\pi^+ \pi^+$ , we consider the consequences of the strong  $\pi^+ \pi^+$  decay which accounts for almost the entire decay width of the meson. With the empirical value of decay width, one can define a vertex which then leads naturally to the two-pion exchange mechanism illustrated in Fig. 2 with  $M = \pi^+$  in the intermediate state. Clearly, this two-pion exchange mechanism is a part of the one-loop corrections discussed in Ref. [17] for  $\pi^+$  photoproduction. A more complete calculation of one-loop corrections to photoproduction is accomplished in this work by including also the intermediate  $\pi^+ N$  state. Details will be given in Section II F.

The  $f_2$  exchange model for photoproduction was motivated by the results from the analyses of  $pp$  scattering data [24]. In the study of  $pp$  scattering the secondary Regge trajectory is represented by the  $f$  trajectory, and the idea of Pomerion- $f$  proportionality had been used to model the Pomerion couplings using the  $f_2$  couplings until 1970's [25{28]

before the soft Pomeron model of Donnachie and Landshoff [29]. By considering the role of the  $f_2$  trajectory in  $pp$  scattering, it is natural to consider the  $f_2$  exchange model for vector meson photoproduction. However, the  $f_2$  exchange model developed in Refs. [9, 21] for

photoproduction used the Pomeron- $f$  proportionality in the reverse direction. Namely, they assume that the structure of the  $f_2$  couplings are the same as that of the soft Pomeron exchange model. Thus the  $f_2$  tensor meson was treated as a  $C = +1$  isoscalar photon, i.e. a vector particle. In addition, the fit to the data is achieved by introducing an additional adjustable parameter to control the  $f_2$  coupling constants [9]. In this work, we elaborate an  $f_2$  exchange model starting from effective Lagrangians constructed by using the empirical information about the tensor properties of the  $f_2$  meson. The main objective of this work is to construct a model including this newly constructed  $f_2$  exchange amplitude and explicit two-pion exchange amplitude discussed above.

This paper is organized as follows. In Section II, we explicitly define the amplitudes for the considered photoproduction mechanisms, including the Pomeron exchange,  $f_2$  exchange, pseudoscalar meson exchanges,  $s$ - and  $u$ -channel nucleon terms, and the newly constructed  $f_2$  exchange. The  $2^+$  exchange amplitudes are then given to complete our model construction. The numerical results are presented in Section III. We consider calculations from two models. Both models contain the  $s$ - and  $u$ -channel nucleon terms and the exchanges of Pomeron,  $f_2$ , and  $f_0$ . The first model includes the  $f_2$  exchange, while the second model includes the two-pion exchange and  $f_2$  exchange. We explore the extent to which these two rather different models can be distinguished by examining the differential cross sections and spin asymmetries. Section IV contains a summary and discussions. The details on the  $f_2$  interactions with the photon and hadrons are given in Appendix.

## II. MODELS FOR PHOTOPRODUCTION

In this Section, we discuss possible production mechanisms for  $p^+ p^-$ . We first discuss single particle exchanges as depicted in Fig. 1. Then the  $2^+$  exchange model will be constructed. Each of the considered production amplitude, as illustrated in Fig. 1, can be written as

$$T_{fi} = " (V)M" ( ); \quad (1)$$

where " $(V)$ " and " $( )$ " are the polarization vectors of the vector meson and the photon, respectively. We denote the four-momenta of the initial nucleon, final nucleon, incoming photon, and outgoing vector meson by  $p, p^0, k$ , and  $q$ , respectively. The Mandelstam variables are  $s = W^2 = (k + p)^2$ ,  $t = (p - p^0)^2$ , and  $u = (p - q)^2$ .

### A. Pomeron exchange

We first consider the Pomeron exchange depicted in Fig. 1(a). In this process, the incoming photon first converts into a  $q\bar{q}$  pair, which interacts with the nucleon by the Pomeron exchange before forming the outgoing vector meson. The quark-Pomeron vertex is obtained by the Pomeron-photon analogy [29], which treats the Pomeron as a  $C = +1$  isoscalar photon, as suggested by a study of nonperturbative two-gluon exchanges [30]. We then have [29, 31{33]

$$M_P = G_P(s; t) T_P; \quad (2)$$

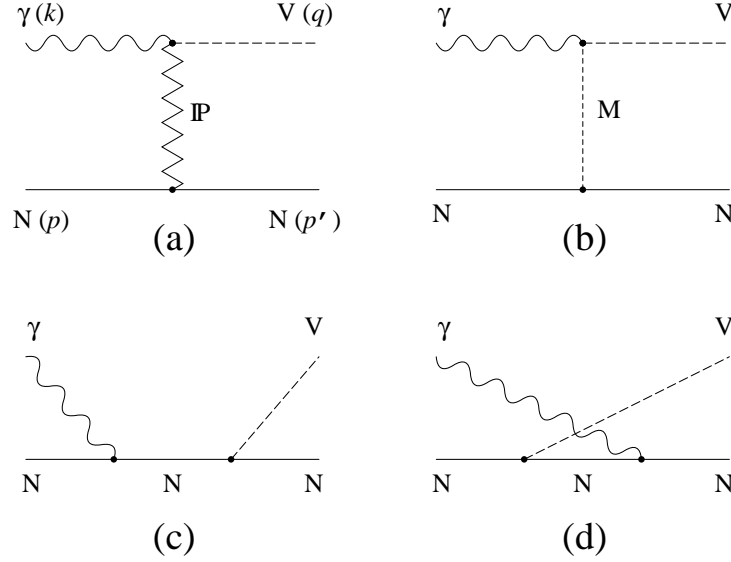


FIG. 1: Models for photoproduction. (a,b) t-channel Pomeron and one-meson exchanges ( $M = f_2$ ;  $\pi$ ;  $\rho$ ). (c,d) s- and u-channel nucleon pole terms.

with

$$T_P = i12 \frac{p}{4} \frac{M_V^2}{\epsilon_m} \frac{q \cdot q^0}{f_V} \frac{1}{M_V^2 - t} \frac{2 \cdot 2^0}{2^0 + M_V^2 - t} F_1(t) u(p^0) f k \quad g \quad k \quad g u(p); \quad (3)$$

where  $\epsilon_m = e^2 = 4$  and  $F_1$  is the isoscalar electromagnetic form factor of the nucleon,

$$F_1(t) = \frac{4M_N^2}{(4M_N^2 - t)} \frac{2.8t}{(1 - t=0.71)^2}; \quad (4)$$

with  $t$  in  $\text{GeV}^2$ . The proton and vector meson masses are represented by  $M_N$  and  $M_V$ , respectively. ( $M_V = M$  in our case.)

The Regge propagator for the Pomeron in Eq. (2) reads

$$G_P = \frac{s}{s_0} \exp^{-\frac{p}{p}(t-1)} \quad \text{exp} \quad \frac{i}{2} [p(t) - 1] : \quad (5)$$

The Pomeron trajectory is taken to be the usual form  $p(t) = 1.08 + \frac{0}{p} t$  with  $\frac{0}{p} = 1 = s_0 = 0.25 \text{ GeV}^2$  [29]. In Eq. (3),  $f_V$  is the vector meson decay constant:  $f = 5.33$ ,  $f_1 = 15.2$ , and  $f = 13.4$ . The coupling constants  $u = d = 2.07 \text{ GeV}^{-1}$ ,  $s = 1.60 \text{ GeV}^{-1}$ , and  $\frac{2}{0} = 1.1 \text{ GeV}^2$  are chosen to reproduce the total cross section data at high energies,  $E = 10 \text{ GeV}$ , where the total cross section of vector meson photoproductions are completely dominated by the Pomeron exchange. For photoproduction, we set  $q = q^0 = u = d$ .

## B. Meson exchange

The meson exchange model advocated by Friman and Soyeur [19] is based on the observation that  $(\pi^+ \pi^-)$  is the largest among all meson radiative decays, which

leads to the assumption that the photoproduction process at low energies is dominated by the exchange of  $\pi$ . The  $\pi$  is then effectively represented by a meson. The effective Lagrangian for this model reads [8, 19, 20]

$$L = \frac{eg}{M} (\bar{q} \gamma^\mu q A^\nu \gamma_\nu \bar{q} \gamma^\mu q A^\nu) + g_{NN} N^\mu N^\nu; \quad (6)$$

where  $\pi$  is the  $\pi^0$  meson field and  $A$  the photon field. The resulting meson exchange amplitude is

$$M = \frac{eg g_{NN}}{M} \frac{1}{t - M^2} (k_{q\bar{q}} \bar{q} q k_{\bar{q}q} \bar{q} q) u(p^0) u(p) F_{NN}(t) F(t); \quad (7)$$

where

$$F_{NN}(t) = \frac{2 - M^2}{2 - t}; \quad F(t) = \frac{2 - M^2}{2 - t} \quad (8)$$

are the form factors. The cut parameters of the form factors and the product of coupling constants  $g g_{NN}$  are adjusted to fit the photoproduction data at low energies. It was found [19, 20] that

$$\begin{aligned} M &= 0.5 \text{ GeV}; & g_{NN}^2 &= 4 = 8.0; & g &= 3.0; \\ &= 1.0 \text{ GeV}; & & & &= 0.9 \text{ GeV}; \end{aligned} \quad (9)$$

The resulting mass parameter is close to the value  $M = 0.55 - 0.66 \text{ GeV}$  of Bonn potential [34]. If we further take the value  $g_{NN}^2 = 4 = 8.3 - 10$  from Bonn potential, we then find that the resulting  $g$  is close to the values from the QCD sum rules,  $g_{(QCD SR)} = 3.2 - 0.6$  [35] or  $2.2 - 0.4$  [36]. However such a large value of  $g$  corresponds to a  $\pi^0 \pi^0 \pi^0$  decay width that is about a factor of 30 larger than the empirical value of  $(\pi^0 \pi^0 \pi^0)$  [22, 37]. If we accept the empirically estimated value of SND experiment [37],  $BR(\pi^0 \pi^0 \pi^0) = (1.9^{+0.9}_{-0.8} \cdot 0.4) \cdot 10^{-5}$ , which means  $(\pi^0 \pi^0 \pi^0) = 2.83 \text{ keV}$ , we get

$$g = 0.25; \quad (10)$$

since the Lagrangian (6) gives

$$(\pi^0 \pi^0 \pi^0) = \frac{eg^2}{24M^5} M^2 M^2 M^3; \quad (11)$$

This value is smaller than that of Eq. (9) by an order of magnitude. Therefore, the exchange models suffer from the big uncertainty of  $g$ , which is under debate [22, 23, 37, 38]. Furthermore, there is no clear particle identification of a  $\pi$  particle and the use of exchange in defining  $NN$  potential has been seriously questioned. Thus it is possible that the exchange may not be the right mechanism for photoproduction.

### C. Pseudoscalar meson exchanges

The and meson exchanges are also allowed for photoproduction, although their contributions are known to be not important. They are calculated from

$$\begin{aligned} L_\pi &= \frac{eg'}{M_V} (\bar{q} \gamma^\mu q A^\nu \gamma_\nu \bar{q} \gamma^\mu q A^\nu); \\ L_{\pi\pi} &= \frac{g_{\pi\pi}}{2M_N} N^\mu N^\nu; \end{aligned} \quad (12)$$

where  $\gamma' = \gamma^0$ ;  $\gamma$ . The coupling constants  $g_{\gamma'}$  are fixed by the  $\pi^0 \pi^0 \pi^0$  decay widths

$$(\pi^0 \pi^0 \pi^0) = \frac{e \gamma g^2}{24 M_V^5} (M_V^2 - M_\pi^2)^3; \quad (13)$$

Using the experimental data [39],  $(\pi^0 \pi^0 \pi^0)_{\text{expt.}} = 121 \pm 31 \text{ keV}$  and  $(\pi^0 \pi^0 \pi^0)_{\text{expt.}} = 62 \pm 17 \text{ keV}$ , we get

$$g_{\gamma'} = 0.756; \quad g_{\gamma} = 1.476; \quad (14)$$

This also gives  $g_{\pi^0} = 1.843$  and  $g_{\pi^0} = 0.414$ . We use  $g_{\pi \pi}^2 = 4 = 14.3$  and the SU(3) relation to get  $g_{\pi \pi}^2 = 4 = 0.99$ , albeit there are other estimates on the value of  $g_{\pi \pi}$  reported in the literature.

The pseudoscalar meson exchange production amplitude, Fig. 1(b), calculated from the Lagrangian (12) reads

$$M_{\pi^0} = \frac{ieg_{\pi^0} g_{\pi \pi}}{2M_N M_V} \frac{1}{t - M_\pi^2} \quad q \cdot k \cdot u(p^0) \quad (p^0 \bar{p}^0) u(p) F_{\pi \pi}(t) F_{\pi^0 \pi^0}(t); \quad (15)$$

where the form factors are

$$F_{\pi \pi}(t) = \frac{2, -M_\pi^2}{t^2 - t}; \quad F_{\pi^0 \pi^0}(t) = \frac{2, -M_\pi^2}{t^2 - t}; \quad (16)$$

We use  $M_N = 0.6 \text{ GeV}$ ,  $M_V = 0.77 \text{ GeV}$ ,  $M_\pi = 1.0 \text{ GeV}$ , and  $M_{\pi^0} = 0.9 \text{ GeV}$  [13, 19].

#### D. Nucleon pole terms

The s- and u-channel nucleon terms, Fig. 1(c,d), are calculated from

$$L_{pp} = eN_A \frac{p}{2M_N} @ A_N; \\ L_{pp} = g_{\pi \pi} N \frac{p}{2M_N} @ N; \quad (17)$$

The resulting production amplitude is

$$M_N = \frac{eg_{\pi \pi}}{2} u(p^0) \frac{h}{v(q)} \frac{p + k + M_N}{s - M_N^2} @ (k) F_N(s) \\ + (k) \frac{p - q + M_N}{u - M_N^2} \frac{i}{v(q)} F_N(u) u(p); \quad (18)$$

where

$$v = \frac{i}{2M_N} q; \quad = + \frac{i}{2M_N} k; \quad (19)$$

The form factor has the form [40]

$$F_N(r) = \frac{4}{\frac{4}{N} + (r - M_N^2)^2}; \quad (20)$$

with  $N = 0.5$  GeV taken from Refs. [8, 13]. This choice of the nucleon form factor leads to a satisfactory explanation of the steep rise of the differential cross sections with increasing  $|t|$  in terms of the  $u$ -channel nucleon term [Fig. 1(d)].

Because  $F_N(s) \neq F_N(u)$ , the above amplitude does not satisfy the gauge invariance. In order to restore the gauge invariance, we project out the gauge non-invariant terms as

$$v \cdot \frac{k}{k} q \cdot q \cdot v; \quad ! \cdot \frac{k}{q} q \cdot k \cdot : \quad (21)$$

For the  $NN$  coupling constants, we take the values determined in the analyses of pion photoproduction and  $N$  scattering [41]:

$$g_{NN} = 62; \quad = 1.0; \quad (22)$$

and the anomalous magnetic moment of the nucleon is  $\gamma_p = 1.79$ .

#### E. $f_2$ meson exchange

We now discuss the exchange of the  $f_2(1270)$  tensor meson, which has quantum numbers  $I^G(J^{PC}) = 0^+(2^{++})$ . The mass and decay width of the  $f_2(1270)$  are  $M_f = 1275.4 \pm 1.2$  MeV and  $(f_2) = 185.1^{+3.4}_{-2.6}$  MeV [39]. Because of its quantum numbers, it has been once suggested as a candidate for the Pomeron. But this assumption violates the duality with the  $a_2$  trajectory which includes  $I^G(J^{PC}) = 1^-(2^{++})$  state and it is now believed that the  $f_2$  does not lie on the Pomeron trajectory.

In the approach of Ref. [9], the  $f_2$  is treated as a  $C = +1$  isoscalar photon just like the Pomeron. This leads to a Regge amplitude of the following form

$$M_{f_2} = f_2 G_{f_2}(s; t) T_p; \quad (23)$$

where<sup>1</sup>

$$G_{f_2}(s; t) = \frac{s}{s_1} \frac{f_2(t)^{-1}}{2 \sin[f_2(t)]} \frac{(1 + \exp[i f_2(t)])^0}{[f_2(t)]}; \quad (24)$$

with  $s_1 = 1 = \frac{0}{f_2} 1$  GeV<sup>2</sup>, while the form of  $T_p$  is the same as given in Eq. (3). The  $f_2$  trajectory is linearly approximated as  $f_2(t) = 0.47 + 0.89t$  [21, 24]. In order to control the strength of the  $f_2$  coupling to the hadrons, a free parameter  $f_2$  was introduced [9] and adjusted to fit the photoproduction data at low energies.

In this paper, we depart from this Regge parameterization and construct an  $f_2$  exchange model solely based on the tensor structure of the  $f_2$  meson. We will use the experimental data associated with the  $f_2$  meson, the tensor meson dominance, and vector meson dominance

<sup>1</sup> The form of  $G_{f_2}$  in Eq. (24) is due to the fact that the  $f_2$  interaction is treated as that of an isoscalar photon, i.e., a vector particle interaction. If we use the tensor structure of the  $f_2$  interaction, it would be

$$G_{f_2}(s; t) = \frac{s}{s_1} \frac{f_2(t)^{-2}}{2 \sin[f_2(t)]} \frac{(1 + \exp[i f_2(t)])^0}{[f_2(t)]^1};$$

$G_{fNN}^2 = 4$	$F_{fNN} = G_{fNN}$	
1:12		Ref. [42]
3:31	0	Ref. [45]
3:31	0:63	0:06 0:17
4:0	1:0	0:00 0:07
2:2	0:9	0:6 0:9
0:38	0:04	0
		Ref. [44]

TABLE I: Estimates on the  $f_{2N}$  coupling constants,  $G_{fNN}$  and  $F_{fNN}$ , using  $N$  dispersion relations. The values are compared with the prediction of tensor meson dominance [44].

assumptions to fix the  $f_2$  coupling constants, such that the strength of the resulting  $f_2$  exchange amplitude is completely fixed in this investigation. Following Refs. [42, 43], the effective Lagrangian accounting for the tensor structure of the  $f_2NN$  interaction reads<sup>2</sup>

$$L_{fNN} = 2i \frac{G_{fNN}}{M_N} N (\partial + \partial) N f + 4 \frac{F_{fNN}}{M_N} \partial N \partial N f ; \quad (25)$$

where  $f$  is the  $f_2$  meson field. This gives the following form of the  $f_{2N}$  vertex function,

$$V_{\text{beld}} = u(p_d) \frac{G_{fNN}}{M_N} [ + ] + \frac{F_{fNN}}{M_N^2} u(p_d); \quad (26)$$

where  $\partial = (p_b + p_d)$ ,  $p_b$  and  $p_d$  are the incoming and outgoing nucleon momentum, respectively, and  $u$  is the polarization tensor of the  $f_2$  meson.

The coupling constants associated with the  $f_2$  meson were first estimated by using the dispersion relations to analyze the backward  $N$  scattering [42] and the  $^3N\bar{N}$  partial-wave amplitudes. The results are summarized in Table I. Note that the value estimated based on the tensor meson dominance [44] is much smaller than the empirical values. (See Appendix for details.)

The most general form for the  $fV$  vertex satisfying gauge invariance reads [49]

$$h(k)V(k^0) f_2 i = \frac{1}{M_f} \partial^0 f A^{fV}(k; k^0); \quad (27)$$

where  $\partial$  and  $\partial^0$  are the polarization vectors of the photon and the vector meson, respectively, and

$$\begin{aligned} A^{fV}(k; k^0) = & \frac{f_{fV}}{M_f^3} [g(k \cdot k - k^0 \cdot k)](k - k^0) (k - k^0) \\ & + g_{fV} [g(k - k^0) (k - k^0) + g(k^0 \cdot k - k^0) + g(k^0 \cdot k - k^0) \\ & - g(k \cdot k - k^0) - g(k \cdot k - k^0) - 2k \cdot k(g \cdot g + g \cdot g)]; \end{aligned} \quad (28)$$

The tensor meson dominance together with the vector meson dominance gives [49]

$$f_{fV} = 0 \quad \text{and} \quad g_{fV} = \frac{e}{f_V} G_{fVV}; \quad (29)$$

<sup>2</sup> In the conventions of Ref. [43],  $G_{fNN}^{(1)} = G_{fNN}$  and  $G_{fNN}^{(2)} = F_{fNN}$ .

where

$$G_{fVV} = G_f = 5:76; \quad (30)$$

Here  $G_f$  is determined from the decay width of  $f_2$  ! . The details on the  $f_2$  interactions with the photon and hadrons, and tensor meson dominance are given in Appendix.

With the above formulas, it is straightforward to obtain the production amplitude as

$$M_{f_2} = u(p) \langle p; p^0 \rangle u(p) \frac{P}{(p - p^0)^2} ; \quad M_f^2 V ; \quad (k; q) F_{fNN}(t) F_{fV}(t); \quad (31)$$

where

$$\begin{aligned} \langle p; p^0 \rangle &= \frac{G_{fNN}}{M_N} [(p + p^0) + (p + p^0)] + \frac{F_{fNN}}{M_N^2} (p + p^0) (p + p^0); \\ P &= \frac{1}{2} (g_g + g_g) - \frac{1}{3} g_g; \\ V &= \frac{f_{fV}}{M_f^4} [g(k - q) + qk] (k + q) (k + q) \\ &+ \frac{g_{fV}}{M_f} \frac{h}{g} (k + q) (k + q) - gq (k + q) - gq (k + q) \\ &- gk (k + q) - gk (k + q) + 2kq (g_g + g_g); \quad (32) \end{aligned}$$

and

$$g = g + \frac{\langle p - p^0 \rangle \langle p - p^0 \rangle}{M_f^2}; \quad (33)$$

The form factors are chosen as

$$F_{fNN}(t) = \frac{\frac{2}{f_{fNN}} M_{f_2}^2}{t}; \quad F_{fV}(t) = \frac{\frac{2}{f_{fV}} M_{f_2}^2}{t}; \quad (34)$$

## F. 2 exchange

In this subsection, we discuss the 2 exchange for photoproduction as shown in Fig. 2. For the intermediate baryon state we consider the nucleon state only, and and ! are considered for the intermediate meson. Intermediate and are not allowed since and vertices are forbidden by G parity. We compute the loop amplitude of Fig. 2 by making use of the method of Sato and Lee [41], which gives

$$T_{loop} = d^3 q^0 B_{NNM} (k; q^0; E) G_{MN} (q^0; E) V_{MN; N} (q^0; q; E); \quad (35)$$

where

$$G_{MN} (q^0; E) = \frac{1}{E - E_N (q^0) - E_M (q^0) + i}; \quad (36)$$

for  $(M N) = (N)$  and  $(!N)$ .

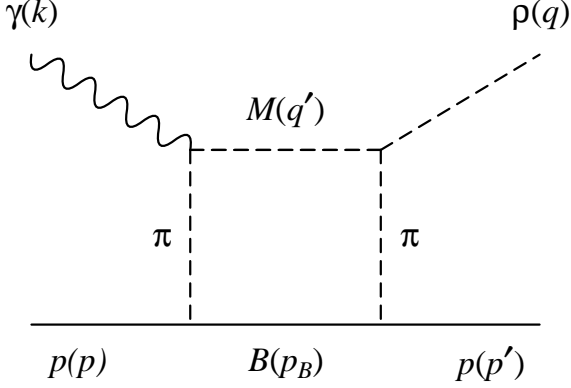


FIG. 2: 2 exchange in photoproduction. The intermediate meson state ( $M$ ) includes  $\pi$ ,  $\rho$ , and  $\omega$ , and the baryon ( $B$ ) includes the nucleon.

Equation (35) can be rewritten as

$$T_{\text{loop}} = \frac{Z}{P} \int \frac{d^3 q^0}{W} \frac{V(q^0; q) B(k; q^0)}{E_B(q^0) E_M(q^0)} \int d_{k_t \in B_M}(k_t) V(k_t; q) B(k; k_t) (W - M_M - M_B); \quad (37)$$

where  $\Theta(x)$  is the step function and

$$B_M(k) = \frac{k E_B(k) E_M(k)}{E_B(k) + E_M(k)}; \quad (38)$$

Through the on-shell condition  $W = E_B(k_t) + E_M(k_t)$ ,  $k_t$  is determined as

$$k_t = \frac{1}{2W} \sqrt{W^2 - M_M^2 - M_B^2}; \quad (39)$$

where

$$(x; y; z) = x^2 + y^2 + z^2 - 2(xy + yz + zx); \quad (40)$$

For the intermediate  $N$  channel, the 2 exchange amplitude can be calculated from

$$\begin{aligned} L &= e \Theta(k_3 A); \\ L &= g (\Theta(k_3 A)); \\ L_{NN} &= \frac{g_{NN}}{2M_N} N_5 \Theta(N); \end{aligned} \quad (41)$$

The coupling constant  $g$  is determined from the decay width ( $\Gamma$ ), which reads

$$(\Gamma) = \frac{g^2}{48 M^2} M^2 - 4M^2 \stackrel{3=2}{=} ; \quad (42)$$

Using  $(\Gamma) = 150.7 \text{ MeV}$  [39], we obtain

$$g = 6.04; \quad (43)$$

Then the 2-exchange transition amplitude with intermediate  $N$  channel reads

$$\begin{aligned} M_{NN} &= V(q^0; q) B(k; q^0) \\ &= \frac{1}{(2\pi)^3 E_N(p_B)} \frac{1}{2E(q^0)} \frac{eg g_{NN}^2}{4M_N^3} (q^0 \cdot p_B + p^0) (p_B \cdot p \cdot q^0) \\ &\quad \frac{1}{(p_B \cdot p)^2} \frac{1}{M^2} \frac{1}{(p_B \cdot p^0)^2} \frac{1}{M^2} u(p^0) u(p); \end{aligned} \quad (44)$$

where

$$= (p \cdot p_B) (p_B \cdot M_N) (p \cdot p); \quad (45)$$

The loop integration must be regularized by introducing form factors. We include the form factors for  $\gamma$ ,  $\gamma$ , and  $NN$  vertices. In addition, we also introduce the form factor to take into account the on-shellness of the intermediate states,

$$F \cdot (q^0) = \frac{\gamma^2 + k_t^2}{\gamma^2 + q^2} \quad : \quad (46)$$

Thus the final form of the form factor is

$$F = F \cdot (q^0) F_{NN}(t_1) F_{NN}(t_2) F_{NN}(t_1) F_{NN}(t_2); \quad (47)$$

where

$$F_{NN}(t) = \frac{2}{2} \frac{M^2}{t}; \quad F_{NN}(t) = \frac{2}{2} \frac{M^2}{t}; \quad (48)$$

and  $t_1 = (p_B \cdot p)^2$  and  $t_2 = (p_B \cdot p^0)^2$ .

The 2-exchange amplitude with intermediate  $1N$  channel is computed from  $L_{NN}$  of Eq. (41) and

$$\begin{aligned} L_V &= \frac{eg!}{M!} \quad @! @A^0; \\ L_{VV} &= g_{VV} \quad \text{Tr}(@! @); \end{aligned} \quad (49)$$

where

$$= = p \frac{0}{2} \frac{p}{2} + \frac{0}{0}; \quad = = p \frac{0}{2} \frac{p}{2} + \frac{0}{0}; \quad : \quad (50)$$

The hidden gauge approach, for example, gives [50]

$$g_{VV} = \frac{3g^2}{8^2 f}; \quad (51)$$

where  $f = 93$  MeV. Since vertex is not allowed by  $G$  parity, we can have  $1N$  intermediate channel only. With the above effective Lagrangians, we obtain the 2-exchange amplitude with intermediate  $1N$  channel as

$$\begin{aligned} M_{1N} &= \frac{1}{(2\pi)^3 E_N(p_B)} \frac{1}{2E(q^0)} \frac{eg_{VV} g! g_{NN}^2}{4M! M_N^3} \\ &\quad \frac{1}{(p_B \cdot p)^2} \frac{1}{M^2} \frac{1}{(p_B \cdot p^0)^2} \frac{1}{M^2} u(p^0) u(p); \end{aligned} \quad (52)$$

where is defined in Eq. (45).

### III. CROSS SECTIONS AND POLARIZATION ASYMMETRIES

In this work we first re-examine the commonly employed exchange by considering Model (A) which includes the Pomeron,  $f_2$ ,  $2$  exchanges, and the s- and u-channel nucleon terms. We then explore Model (B) which is constructed by replacing the exchange in Model (A) by the  $f_2$  and  $2$  exchanges. All parameters of the models are explained in Section II. In particular, the exchange parameters are given in Eq. (9). For the  $f_2$  exchange, we use (see Appendix)

$$G_{f_{NN}}^2 = 4 = 2.2; \quad F_{f_{NN}} = 0; \quad G_{f_{VV}} = 5.76; \quad (53)$$

with the relation (29). The only unspecified parameters are the cut parameters  $f_{NN}$  and  $f_{VV}$  for the  $f_2$  exchange and the parameter  $\lambda$  of Eq. (46) for regularizing the loop integrations. The parameter  $\lambda$  for all loop integrations is fixed to be 0.50 GeV which is identical to the value used in our previous investigation [17] of the one-loop corrections on  $\pi^+ p$  photoproduction. The other two parameters of Model (B) are adjusted to fit the cross section data and are found to be

$$f_{NN} = f_{VV} = 1.4 \text{ GeV}; \quad (54)$$

This is an unsatisfactory aspect of this work, but it is unavoidable in any phenomenological approach. Future theoretical calculations of form factors are therefore highly desirable.

The differential cross sections for  $p^+ p$  calculated from Model (A) are compared with the SLAC data [51] and the recent CLAS data [3] in Fig. 3. We see that the full calculations (solid curves) are dominated by the exchange contributions (dot-dashed curves). The contributions from the other exchange mechanisms (dashed curves) become comparable only in the very forward and backward angles. This is mainly due to the fact that the Pomeron exchange [Fig. 1(a)] is forward peaked and the u-channel nucleon term [Fig. 1(d)] is backward peaked. It is clear that the data can only be qualitatively reproduced by Model (A). The main difficulty is in reproducing the data in the large  $|t|$  (larger than about 3 GeV $^2$ ) region. No improvement can be found by varying the cut parameters of various form factors of Model (A) which includes the commonly used exchange.

The differential cross sections calculated from Model (B) are shown in Fig. 4. The solid curves are the best fits to the data we could obtain by choosing the cut parameters given in Eq. (53) for the  $f_2$  exchange. In the same figures, we also show the contributions from the  $f_2$  exchange (dot-dashed curves),  $2$  exchange (dashed curves), and the rest of the production mechanisms (dotted curves). It is interesting to note that the  $f_2$  exchange (dot-dashed curves in Fig. 4) drops faster than the exchange (dot-dashed curves in Fig. 3) as  $t$  increases. On the other hand, the  $2$  exchange (dashed curves in Fig. 4) gives a significant contribution in large  $|t|$  region. Thus the sum of the  $f_2$  exchange and  $2$  exchange is comparable to the commonly used exchange in fitting the data. However, Model (B) also cannot fit the data at large  $|t|$  (larger than 3 GeV $^2$ ). But this is expected since we have not included N and  $\pi^0$  excitation mechanisms which were found [13] to give significant contributions to  $\pi^+ p$  photoproduction at large  $|t|$ . However, we will not address this rather non-trivial issue here. Instead we focus on exploring the differences between Model (A) and (B) in the small  $t$ , namely  $|t| < 2 - 3$  GeV $^2$  region, where both models can describe the differential cross section data to some extent.

The full calculations of the  $p^+ p$  differential cross sections from Model (A) and (B) are compared in Fig. 5. From those figures, one may argue that Model (B) is slightly better in small  $t$  region. However, it would be rather fair to say that the two models are

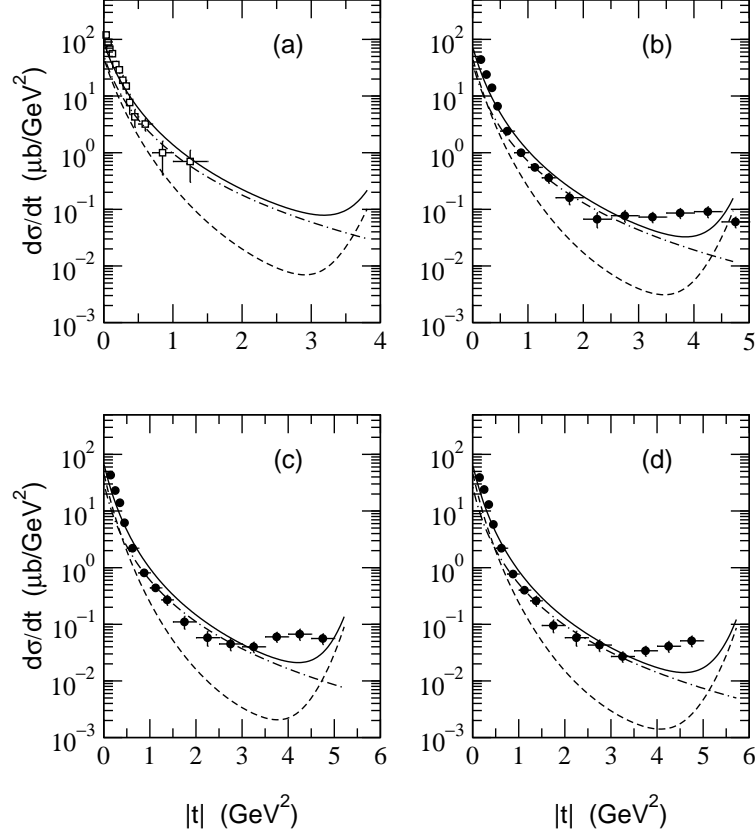


FIG. 3: Differential cross sections of Model A at  $E =$  (a) 2.8, (b) 3.28, (c) 3.55, and (d) 3.82 GeV. The dot-dashed lines are from exchange and the dashed lines are without exchange. The solid lines are the full calculation. Experimental data are from Ref. [51] (open squares) and Ref. [3] (filled circles).

comparable in reproducing the data. We therefore explore their differences in predicting the spin asymmetries, which are defined, e.g., in Ref. [33]. The results for the single spin asymmetries are shown in Fig. 6 for  $E = 3.55$  GeV. Clearly the single spin asymmetries including the target asymmetry  $T_y$  and the recoiled proton asymmetry  $P_y$  would be useful to distinguish the two models and could be measured at the current experimental facilities. Of course our predictions are valid mainly in the small  $t$  region since the  $N$  excitations, which are expected to be important at large  $t$  [13], are not included in this calculation.

Our predictions on the beam-target and beam-recoil double asymmetries [33] are given in Fig. 7. Here we again see significant differences between the two models in the region of small  $t$ . Experimental tests of our predictions given in Figs. 6 and 7 will be useful in understanding the non-resonant mechanisms of photoproduction.

Since both the  $f_0$  and  $f_2$  exchanges are natural parity exchanges, it would be difficult to test them using parity asymmetry or photon asymmetry that can be measured from the decay distribution of the  $\pi$  meson produced by polarized photon beam. For completeness, we give the predictions of the two models on these asymmetries in Fig. 8. As expected, it is very hard to distinguish the two models in the forward scattering angles with these asymmetries.

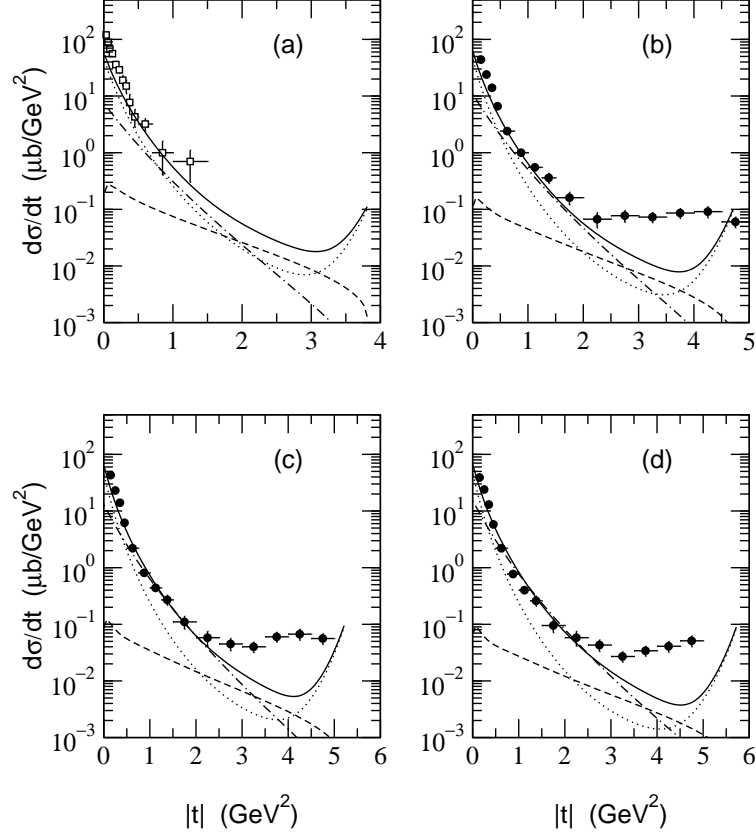


FIG. 4: Differential cross sections of Model (B) at  $E =$  (a) 2.8, (b) 3.28, (c) 3.55, and (d) 3.82 GeV. The dot-dashed lines are from  $f_2$  exchange, the dashed lines are from  $2$  exchange, and the dotted lines are from the other processes, i.e., without  $f_2$  and  $2$  exchanges. The solid lines are the full calculation. Experimental data are from Ref. [51] (open squares) and Ref. [3] (filled circles).

#### IV. DISCUSSION

In this paper, we develop a model for photoproduction by including  $f_2$  and  $2$  exchanges. First the tensor structure of the  $f_2$  interactions with hadrons is explicitly taken into account in the production amplitude. This is very different from the model of Laget [9], where the  $f_2$  interaction structure was borrowed from that of Pomeron exchange assuming Pomeron-f proportionality, i.e.,  $f_2$ -photon analogy. The couplings of  $f_2$  interaction with the hadrons are estimated from NN dispersion relations and using tensor meson dominance together with vector meson dominance. We then include  $2$  exchanges in the production mechanism with the intermediate N and  $^1N$  channels, of which important role is indicated by the large decay width of  $^1N$ . We found that the  $2$  exchange is comparable to  $f_2$  exchange at moderately large  $|t|$ , but suppressed at small  $|t|$ . Therefore, although it shows exponential decrease with increasing  $|t|$ , the  $2$  exchange decreases much slower than the  $f_2$  exchange so that the  $2$  exchange has smaller slope in differential cross sections.

The results are compared with the commonly used exchange model [19]. Although this model suffers from the uncertainty of the coupling  $g$ , it can describe the differential cross section data up to  $|t| = 2-3 \text{ GeV}^2$ . Since the two models are comparable to each other, we have to rely on the spin asymmetries to distinguish them. Because both the  $f_2$  and  $f_2$

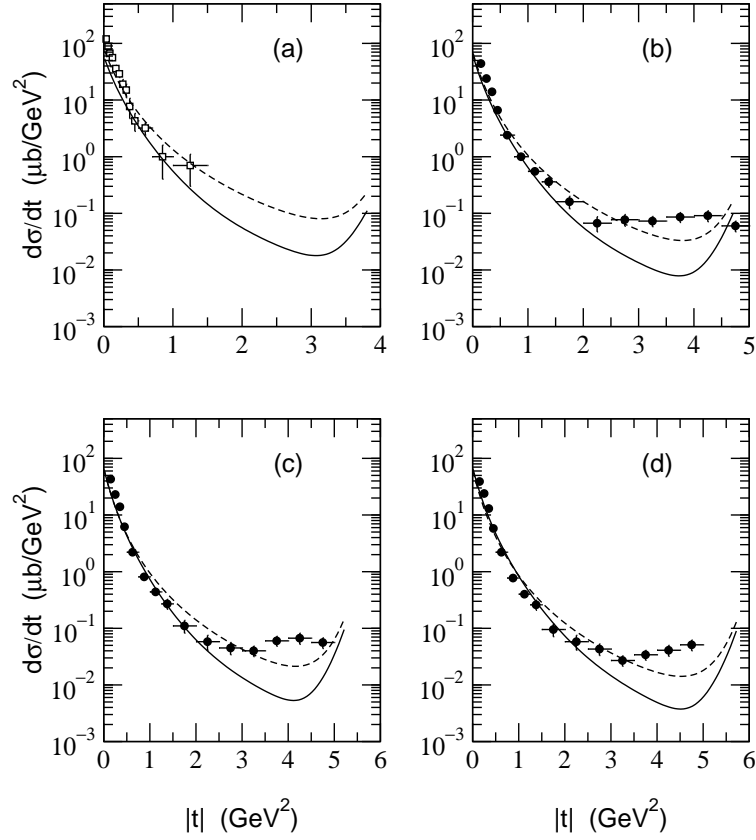


FIG. 5: Differential cross sections of Model (A) and (B) at  $E = 3.55$  GeV. The dashed line is the result of model (A) and the solid line is that of model (B). Experimental data are from Ref. [3].

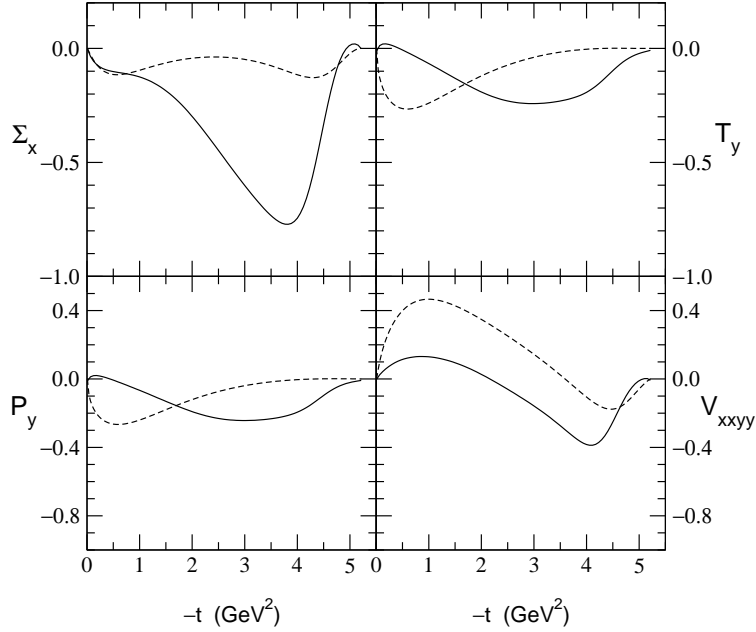


FIG. 6: Single spin asymmetries of Model (A) and (B) at  $E = 3.55$  GeV. Notations are the same as in Fig. 5. The definitions of the spin asymmetries are from Ref. [33].

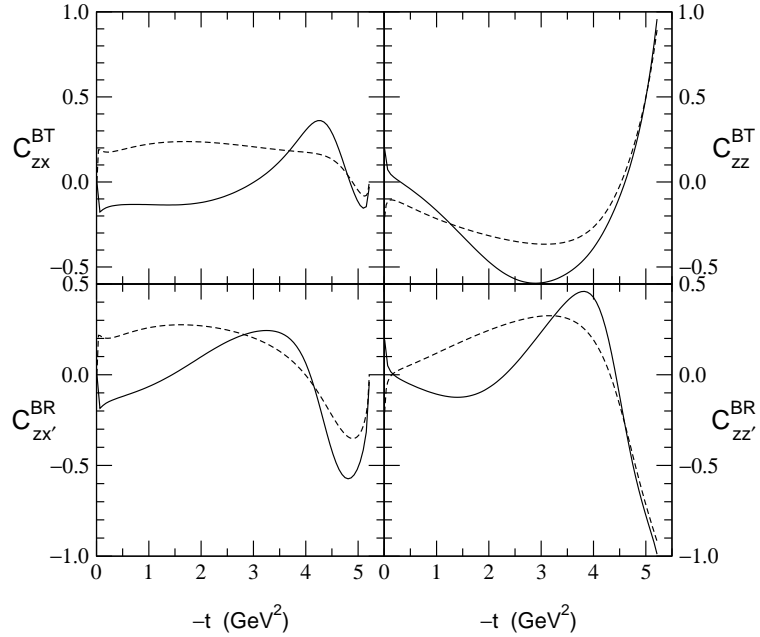


FIG . 7: Double spin asymmetries  $C_{zx}^{BT}$ ,  $C_{zz}^{BT}$ ,  $C_{zx}^{BR}$ , and  $C_{zz}^{BR}$  of Model (A) and (B) at  $E = 355$  GeV. Notations are the same as in Fig. 5.

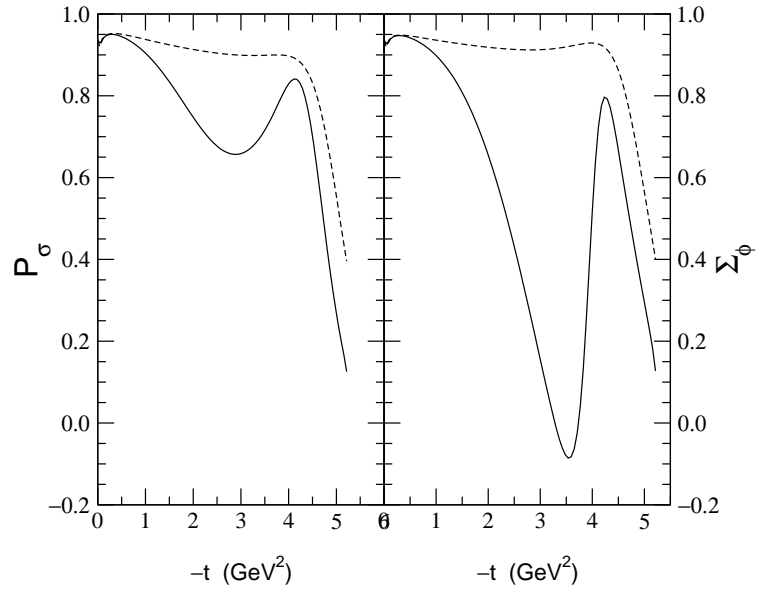


FIG . 8: Spin asymmetries  $P$  and  $W$  of Model (A) and (B) at  $E = 355$  GeV. Notations are the same as in Fig. 5.

exchanges are natural parity exchanges, it is difficult to test them using parity asymmetry or photon asymmetry measured from the decay distribution of the meson produced by polarized photon beam. However, the single spin asymmetries and double spin asymmetries are found to be useful to distinguish the models, especially in the region of forward scattering angles. Therefore, measurements of such quantities would shed light on the understanding of the main non-resonant production mechanisms of photoproduction at low energies. In

addition, the unsatisfactory description of the data at large  $|t|$  would imply the role of the  $N$  and  $\Delta$  resonances as anticipated from the study on  $\pi^+$  photoproduction [13]. So clear understanding on the non-resonant production processes is crucial to estimate the resonance parameters from photoproduction because the two models considered in this paper show some differences at large  $|t|$  as shown in Fig. 5.

#### Acknowledgments

Y.O. is grateful to the Physics Division of Argonne National Laboratory for the hospitality during his stay. The work of Y.O. was supported by Korea Research Foundation Grant (KRF-2002-015-CP0074) and T.-S.H.L. was supported by U.S. DOE Nuclear Physics Division Contract No. W-31-109-ENG-38.

#### APPENDIX : TENSOR MESON DOMINANCE AND $f_2$ -HADRON INTERACTIONS

The free Lagrangian and the propagator of the tensor meson was studied in Refs. [52{56]. The propagator of the tensor meson which has momentum  $p$  reads

$$G^{;\mu} = \frac{1}{p^2 - M_f^2 + i} P^{;\mu}; \quad (A.1)$$

where  $M_f$  is the tensor meson mass and

$$P^{;\mu} = \frac{1}{2} (g^{\mu\nu} g_{\nu\rho} + g^{\mu\rho} g_{\nu\rho}) - \frac{1}{3} g^{\mu\rho} g_{\nu\rho}; \quad (A.2)$$

with

$$g^{\mu\nu} = g_{\mu\nu} + \frac{p^\mu p^\nu}{M_f^2}; \quad (A.3)$$

#### 1. $f_2$ coupling

The effective Lagrangian for  $f_2$  interaction reads [43]

$$L_f = \frac{2G_f}{M_f} \partial_\mu \partial_\nu f^\mu_\nu; \quad (A.4)$$

where  $f$  is the  $f_2$  meson field. This gives the  $f_2$  vertex function as

$$V_f = \frac{G_f}{M_f} (p_a + p_c) (p_a + p_c)^\mu (f^\nu_\mu); \quad (A.5)$$

where  $p_a$  and  $p_c$  are the incoming and outgoing pion momenta, respectively. The minus sign in the Lagrangian (A.4) is to be consistent with the tensor meson dominance [57]. The Lagrangian (A.4) gives the  $f_2^+$  decay width as

$$(f_2^+ \rightarrow \pi^+ \pi^0) = \frac{G_f^2}{80} M_f \left( 1 - 4 \frac{M_f^2}{M_f^2} \right)^{1/2}; \quad (A.6)$$

Using the experimental data ( $f_2^+ \rightarrow \pi^+ \pi^+ \pi^-$ )<sub>expt.</sub> = 156.9 MeV [39], we obtain

$$\frac{G_f^2}{4} = 2.64; \quad (A.7)$$

which gives  $G_f = 5.76$ .

## 2. Tensor meson dominance

The tensor meson dominance (TMD) is an assumption of meson pole dominance for matrix elements of the energy momentum tensor just as the vector meson dominance (VMD) is a pole dominance of the electromagnetic current. By using TMD, one can determine the universal coupling constant of the  $f_2$  meson from its decay width to two pions, which can then be used to determine the  $f_2 NN$  and  $f_2 VV$  couplings. When combined with VMD, this also allows us to estimate the  $f_2$  and  $fV$  vertices. It is interesting to note that the TMD underestimates the  $f_2 NN$  coupling while it overestimates the  $f_2^+ \rightarrow \pi^+ \pi^+ \pi^-$  decay width. But it shows that the  $f_2$  couplings with hadrons and photon can be understood by TMD and VMD at least qualitatively. Here, for completeness, we discuss the method of Refs. [44, 49] to illustrate how to use TMD to get the  $f_2$ -hadron couplings.

Let us first apply TMD to spinless particles [44, 58]. The energy-momentum tensor between spinless particles can be written as

$$h p j(0) \bar{p}^0 i = F_1(\vec{p}^2) + F_2(\vec{p}^2)(\vec{g}^2); \quad (A.8)$$

with  $\vec{p} = (\vec{p} + \vec{p}^0)$  and  $\vec{g} = (\vec{p} - \vec{p}^0)$ . Then with the covariant normalization one has

$$h p j_{00}(x) d^3 x \bar{p}^0 i = E N_p; \quad (A.9)$$

where  $N_p$  is the normalization constant. By comparing with Eq. (A.8), one can find

$$F_1(0) = \frac{1}{2}; \quad (A.10)$$

Now we define the effective couplings for tensor mesons as

$$h f j(0) \bar{p}^0 i = g_f M_f^3; \quad h p f \bar{p}^0 i = \frac{G_{fpp}}{M_f}; \quad (A.11)$$

where the latter equation is consistent with Eq. (A.5). The pole dominance gives

$$\begin{aligned} h p j \bar{p}^0 i &= \sum_f h p f \bar{p}^0 i h f j \bar{p}^0 i = \frac{1}{M_f^2} \\ &= \sum_f g_f M_f^3 \frac{G_{fpp}}{M_f^2} \frac{1}{M_f^2} \\ &= \sum_f \frac{g_f M_f^2 G_{fpp}}{M_f^2} \frac{1}{3} g^2 + \frac{1}{3} \frac{1}{M_f^2} g^2; \end{aligned} \quad ! \quad (A.12)$$

which leads to

$$F_1(-^2) = \frac{X}{f} \frac{g_f M_f^2 G_{fpp}}{2 M_f^2} : \quad (A.13)$$

Thus we have

$$F_1(0) = \frac{X}{f} g_f G_{fpp} = \frac{1}{2} : \quad (A.14)$$

It should be noted that the sum of Eq. (A.14) contains tensor meson nonet, i.e.,  $f_2(1260)$  and  $f_2^0(1525)$ . But in the case of pion- $f_2$  coupling, if we assume the ideal mixing between  $f_2(1260)$  and  $f_2^0(1525)$ , the  $f_2^0(1525)$  decouples by the OZI rule. Therefore we obtain  $G_{f^0} = 0$ , and the universal coupling constant  $g_f$  is determined as

$$g_f = \frac{1}{2G_f} = 0.087; \quad (A.15)$$

using the value of Eq. (A.7).

With the universal coupling constant  $g_f$  determined above, one can now use it to estimate the  $f_2 NN$  coupling. For this purpose, let us apply TMD to spin-1/2 baryon state. The energy-momentum tensor of the spin-1/2 baryons can be written as

$$\begin{aligned} \text{hpj} (0) \dot{p}^0 i = & u(p) \frac{1}{4} ( \dots + \dots ) F_1(-^2) \\ & + \frac{1}{4M_N} F_2(-^2) + ( \dots g^2 ) F_3(-^2) u(p^0); \end{aligned} \quad (A.16)$$

With the covariant normalization, the conditions

$$\begin{aligned} \text{hpj}_{00}(x) d^3x \dot{p}i &= E N_p; \\ \text{hp}p = 0; s_3 &= +\frac{1}{2} j^R f x_{102}(x) x_{201}(x) g d^3x \dot{p}p = 0; s_3 &= +\frac{1}{2} i = \frac{1}{2} N_p; \end{aligned} \quad (A.17)$$

give

$$F_1(0) = 1; \quad F_2(0) = 0; \quad (A.18)$$

Now using the form for  $f_2 NN$  coupling in Eq. (26), assuming the pole dominance gives the following relations:

$$\begin{aligned} 1 &= 4g_f G_{fNN} \frac{M_f}{M_N} + 4g_{f^0} G_{f^0 NN} \frac{M_{f^0}}{M_N}; \\ 0 &= 4g_f F_{fNN} \frac{M_f}{M_N} + 4g_{f^0} F_{f^0 NN} \frac{M_{f^0}}{M_N}; \end{aligned} \quad (A.19)$$

Again by assuming the decoupling of the  $f_2^0$  from the nucleon coupling, we can have [44]

$$\begin{aligned} G_{fNN} &= \frac{1}{4g_f} \frac{M_p}{M_f} = \frac{G_f}{2} \frac{M_p}{M_f} = 2.12; \\ F_{fNN} &= 0; \end{aligned} \quad (A.20)$$

This gives  $G_{fNN}^2 = 4 \times 0.38 = 1.52$  as shown in Table I, which is smaller than the values estimated by N dispersion relations by an order of magnitude. It should also be noted that the values estimated by N dispersion relations may be affected by the inclusion of other meson exchanges. More rigorous study in this direction is, therefore, highly desirable.

### 3. $f_2VV$ coupling

Before we discuss  $f_2$  and  $f_2V$  couplings, we first apply TM D to  $f_2VV$  coupling, where  $V$  stands for vector mesons. The energy-momentum tensor between identical vector mesons contains six independent matrix elements [49],

$$\begin{aligned} hV j \cdot j V^0 i = & G_1 ( \overset{2}{\square} ) ( \overset{0}{\square} ) + G_2 ( \overset{2}{\square} ) ( \overset{0}{\square} ) \overset{0}{\square} ( \overset{0}{\square} ) \\ & + G_3 ( \overset{2}{\square} ) ( \overset{0}{\square} ) \overset{0}{\square} + ( \overset{0}{\square} ) \overset{0}{\square} + ( \overset{0}{\square} ) \overset{0}{\square} + ( \overset{0}{\square} ) \overset{0}{\square} \\ & + G_4 ( \overset{2}{\square} ) ( \overset{0}{\square} ) \overset{0}{\square} + ( \overset{0}{\square} ) \overset{0}{\square} + ( \overset{0}{\square} ) \overset{0}{\square} + ( \overset{0}{\square} ) \overset{0}{\square} \\ & 2 ( \overset{0}{\square} ) \overset{0}{\square} g \overset{2}{\square} ( \overset{0}{\square} + \overset{0}{\square} ) \\ & + G_5 ( \overset{2}{\square} ) ( \overset{0}{\square} ) ( \overset{0}{\square} ) \overset{2}{\square} g \overset{0}{\square} \\ & + G_6 ( \overset{2}{\square} ) ( \overset{0}{\square} ) \overset{0}{\square} ( \overset{0}{\square} ) \overset{2}{\square} g \overset{0}{\square}; \end{aligned} \quad (A 21)$$

where  $\overset{0}{\square} = (p + p^0)$ ,  $\overset{0}{\square} = (p - p^0)$  and  $\overset{0}{\square}$  are the polarization vectors of  $V$  and  $V^0$ , respectively. Then the conditions like Eq. (A 17) give

$$G_1(0) = \frac{1}{2}; \quad G_3(0) = \frac{1}{2}; \quad (A 22)$$

In the pole model, the form factors  $G_1(\overset{2}{\square})$  and  $G_4(\overset{2}{\square})$  are dominated by tensor meson poles. Because of the symmetry property of the tensor meson, we have generally four  $f_2VV$  coupling vertices:

$$\begin{aligned} hV j \cdot j V^0 i = & \frac{G_1}{M_f} ( \overset{0}{\square} ) ( \overset{0}{\square} f ) + \frac{G_2}{M_f^3} ( \overset{0}{\square} ) \overset{0}{\square} ( \overset{0}{\square} f ) \\ & + \frac{G_3}{M_f} ( \overset{0}{\square} ) \overset{0}{\square} + ( \overset{0}{\square} ) \overset{0}{\square} + ( \overset{0}{\square} ) \overset{0}{\square} + ( \overset{0}{\square} ) \overset{0}{\square} f \\ & + \frac{G_4}{M_f} ( \overset{2}{\square} ) ( \overset{0}{\square} + \overset{0}{\square} ) f; \end{aligned} \quad (A 23)$$

while we have used  $f = f = 0$  in writing the  $G_4$  term. For our later use, an effective vertex  $H(\overset{2}{\square}; p^2; p^0)$  is introduced to replace  $\frac{G_4}{M_f} \overset{2}{\square}$  as [49]

$$H(\overset{2}{\square}; p^2; p^0) = \frac{G_4}{M_f} \overset{2}{\square} + (p^2 + p^0 - 2M_V^2); \quad (A 24)$$

Now we use the pole dominance again using Eq. (A 11) to find

$$G_1(\overset{2}{\square}) = \frac{g_f M_f^2 G_1}{2 - M_f^2}; \quad (A 25)$$

which leads to

$$\frac{1}{2} = g_f G_1; \quad G_3 = -G_1; \quad (A 26)$$

combined with Eq. (A 22). Therefore, with Eq. (A 15) we get

$$G_1 = G_3 = G_f = 5:76; \quad (A 27)$$

The above relation should hold for  $f_2$  and  $f_2^+$ . The SU(3) symmetry and the ideal mixing give

$$G_1(f_2^0) = \frac{p_-}{2} G_1(f_2^-); \quad G_1(f_2^0) = G_1(f_2^+) = 0; \quad (A 28)$$

Note that two couplings  $G_1$  and  $G_3$  are determined by TM D but  $G_2$  and  $G_4$  cannot be estimated without further assumptions.

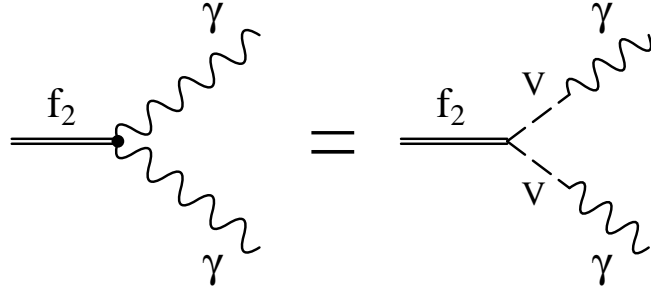


FIG. 9:  $f_2$  ! decay in vector meson dominance.

#### 4. $f_2$ and $f_2 V$ couplings

The remaining two couplings  $G_2$  and  $G_4$  of Eq. (A 23) are estimated by using VMD and gauge invariance. We consider  $f_2$  ! using VMD as illustrated in Fig. 9.

By using  $k = 0$  and VMD, we have

$$\begin{aligned}
 h(k)(k^0) \text{ff} = & \frac{e^2}{(k^2 - M_V^2)(k^2 - M_V^2)} \left( \frac{G_1}{M_f} (0(k-k^0)(k-k^0) f \right. \\
 & \left. + \frac{G_2}{M_f^3} (0(k-k^0)(k-k^0) f \right. \\
 & \left. + \frac{G_3}{M_f} (0(k-k^0)(k-k^0) f \right. \\
 & \left. + (0(k-k^0) + (0(k-k^0) f \right) \\
 & + \frac{G_4}{M_f} [M_f^2 + (k^2 + k^2 - 2M_V^2)](0 + 0) f \quad ; \quad (A 29)
 \end{aligned}$$

where we have introduced the notation

$$G_i = \frac{M_f^2}{f_i^2} G_i^f + \frac{M_f^2}{f_i^2} G_i^{f\perp} ; \quad (A 30)$$

with

$$h_0 \text{ff} = \frac{M_V^2}{f_V} (V) ; \quad (A 31)$$

Because of isospin, there is no mixing between the intermediate and ! mesons. By looking at the amplitude (A 29), however, one can find that it is not gauge invariant, i.e., it does not vanish when replacing  $k$  by  $k$ . This gives a constraint on the couplings. The most general form for  $f_2$  satisfying gauge invariance has two independent couplings as [49]

$$\begin{aligned}
 h(k)(k^0) \text{ff} = & \frac{e^2}{M_V^4} A [(0(k-k^0)(0(k-k^0) f \\
 & + B [(0(k-k^0)(k-k^0) + (0(k-k^0)(0(k-k^0) \\
 & (k-k^0)(0(k-k^0) + (k-k^0)(0(k-k^0) \\
 & 2(k-k^0)(0+0) f \quad ; \quad (A 32)
 \end{aligned}$$

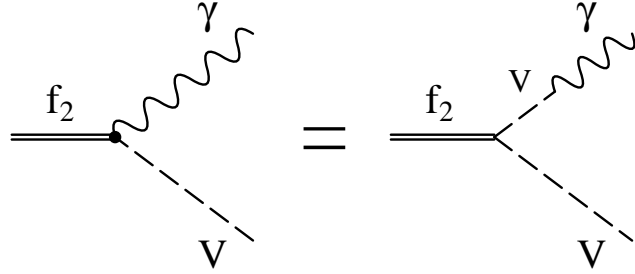


FIG. 10:  $f_2 \rightarrow V \gamma$  decay in vector meson dominance.

which then gives

$$\begin{aligned}
 \frac{G_1}{M_f} &= (k - k^0) A + B; \\
 \frac{G_2}{M_f^3} &= A; \\
 \frac{G_3}{M_f} &= B; \\
 \frac{G_4}{M_f} (M_f^2 + (k^2 + k^0 - 2M_V^2)) &= 2(k - k^0) B = (k^2 + k^0 - M_f^2) B; \quad (A.33)
 \end{aligned}$$

Solving this system at  $k^2 = k^0 = 0$  and  $G_1 = G_3$  gives

$$A = G_2 = 0; \quad (A.34)$$

Since gauge invariance applies to isoscalar and isovector photons separately, we get  $G_2 = 0$  for  $V = \pi$ . Still we do not  $\propto G_4$  and  $\propto$ , but have a constraint,

$$G_4 (M_f^2 + 2 M_V^2) = G_1 M_f^2; \quad (A.35)$$

To complete the model, let us finally consider  $fV$  vertex. Here again, we use the VMD as in Fig. 10. The gauge invariance of the vertex at  $k^2 = M_V^2$  and  $k^0 = 0$  leads to

$$G_4 (M_f^2 + M_V^2) = G_1 (M_f^2 - M_V^2); \quad (A.36)$$

Then solving the coupled equations (A.35) and (A.36) gives [49]

$$G_4 = G_1 \frac{M_f^2 - 2M_V^2}{M_f^2}; \quad = \frac{M_f^2}{M_f^2 - 2M_V^2}; \quad (A.37)$$

Thus we have determined all couplings of Eq. (A.23) with the relation (A.30).

The above procedure shows that the  $f_2$  and  $f_2 V$  vertices can be written with two form factors because of gauge invariance, which read

$$\begin{aligned}
 h(k) (k^0) f_2 i &= \frac{1}{M_f} \delta^0_f A^f(k; k^0); \\
 h(k) V(k^0) f_2 i &= \frac{1}{M_f} \delta^0_f A^{fV}(k; k^0); \quad (A.38)
 \end{aligned}$$

where

$$\begin{aligned}
 A^f(k; k^0) = & \frac{f_f}{M_f^3} [g(k \cdot k - k^0 k) (k \cdot k^0) (k \cdot k^0) \\
 & + g_f [g(k \cdot k^0) (k \cdot k^0) + g(k^0 \cdot k \cdot k^0) + g(k^0 \cdot k \cdot k^0) \\
 & \quad g(k \cdot k^0) g(k \cdot k^0) \\
 & \quad 2k \cdot k(g \cdot g + g \cdot g)]: \quad (A.39)
 \end{aligned}$$

The vertex function  $A^{fv}(k; k^0)$  can be obtained from  $A^f$  by replacing  $f_f$  and  $g_f$  by  $g_{fv}$  and  $g_{fv}$ , respectively.

With Eqs. (A.38) and (A.39), we can obtain the  $f_2^+$  decay width as<sup>3</sup>

$$(f_2^+ \rightarrow \gamma \gamma) = \frac{M_f}{20} \frac{1}{24} f_f^2 + g_f^2 : \quad (A.40)$$

Then TMD and VMD give [49]

$$f_f = 0; \quad g_f = e^2 \frac{1}{f_f^2} + \frac{1}{f_f^2} G_{fvv} : \quad (A.41)$$

The vector meson decay constants are  $f_+ = 5.33$ ,  $f_0 = 15.2$ , and  $f_! = 13.4$ . By noting that TMD gives  $G_{fvv} = G_f$ , we get

$$(f_2^+ \rightarrow \gamma \gamma) = 8.8 \text{ keV} ; \quad (A.42)$$

while its experimental value is  $(f_2^+ \rightarrow \gamma \gamma)_{\text{expt.}} = 2.6 \pm 0.24 \text{ keV}$ . Thus we can find that this procedure overestimates the experimental value by a factor of 3–4.

The decay width of  $f_2^+ \rightarrow VV$  can be computed using Eqs. (A.38) and (A.39) as

$$\begin{aligned}
 (f_2^+ \rightarrow VV) = & \frac{M_f}{10} (1-x)^3 \frac{1}{24} \mathcal{F}_{fv} \mathcal{J}^2 (1-x)^4 (f_{fv} g_{fv} + f_{fv} g_{fv}) \frac{x(1-x)^2}{12} \\
 & + g_{fv} \mathcal{J}^2 1 + \frac{x}{2} + \frac{x^2}{6} ;
 \end{aligned} \quad (A.43)$$

where  $x = M_V^2/M_f^2$ . TMD combined with VDM gives [49]

$$f_{fv} = 0; \quad g_{fv} = \frac{e}{f_V} G_{fvv} : \quad (A.44)$$

This leads to

$$(f_2^+ \rightarrow VV) = (f_2^+ \rightarrow VV) = \frac{g_f^2}{g_f^2} = \frac{f_!^2}{f_+^2} = 8.14 \pm 1.2 \quad (A.45)$$

and [57]

$$(f_2^+ \rightarrow VV) = (f_2^+ \rightarrow VV) = 2 \frac{g_f^2}{g_f^2} (1-x)^3 1 + \frac{x}{2} + \frac{x^2}{6} = 155 : \quad (A.46)$$

---

<sup>3</sup> Here we do not agree with the decay width formula of Ref. [59].

Those quantities are not measured yet.

---

- [1] CLAS Collaboration, E. A. Anzai et al., *Phys. Rev. Lett.* **85**, 4682 (2000).
- [2] CLAS Collaboration, K. Lukashin et al., *Phys. Rev. C* **63**, 065205 (2001); **64**, 059901 (E) (2001).
- [3] CLAS Collaboration, M. Battaglieri et al., *Phys. Rev. Lett.* **87**, 172002 (2001).
- [4] CLAS Collaboration, M. Battaglieri et al., *Phys. Rev. Lett.* **90**, 022002 (2003).
- [5] J. A. Jaka et al., in *Proceedings of 14th International Spin Physics Symposium (SPIN 2000)*, edited by K. Hatanaka, T. Nakano, K. Imai, and H. Eji, (AIP Conf. Proc. 570, 2001), p. 198.
- [6] T. Nakano, in *Proceedings of 14th International Spin Physics Symposium (SPIN 2000)*, edited by K. Hatanaka, T. Nakano, K. Imai, and H. Eji, (AIP Conf. Proc. 570, 2001), p. 189.
- [7] R. W. Clinton, J. B. Dainton, E. Gabathuler, L. S. Littenberg, R. M. Marshall, S. E. Rock, J. C. Thompson, D. L. Ward, and G. R. Brookes, *Phys. Lett.* **64B**, 213 (1976).
- [8] A. I. Titov, T.-S.-H. Lee, H. Toki, and O. Streltsova, *Phys. Rev. C* **60**, 035205 (1999).
- [9] J.-M. Laget, *Phys. Lett. B* **489**, 313 (2000).
- [10] Y. Oh and H. C. Bhang, *Phys. Rev. C* **64**, 055207 (2001).
- [11] Y. Oh, Talk at Symposium for the 30th Anniversary of Nuclear Physics Division of the Korean Physical Society, Seoul, Korea, 2002, to be published in *Jour. Korean Phys. Soc.*, nucl-th/0301011.
- [12] S. Capstick and W. Roberts, *Prog. Part. Nucl. Phys.* **45**, S241 (2000).
- [13] Y. Oh, A. I. Titov, and T.-S.-H. Lee, *Phys. Rev. C* **63**, 025201 (2001).
- [14] Q. Zhao, Z. Li, and C. Bennhold, *Phys. Rev. C* **58**, 2393 (1998).
- [15] Q. Zhao, *Phys. Rev. C* **63**, 025203 (2001).
- [16] A. I. Titov and T.-S.-H. Lee, nucl-th/0305002.
- [17] Y. Oh and T.-S.-H. Lee, *Phys. Rev. C* **66**, 045201 (2002).
- [18] G. Penner and U. Meisel, *Phys. Rev. C* **66**, 055211 (2002).
- [19] B. Friman and M. Soyeur, *Nucl. Phys. A* **600**, 477 (1996).
- [20] Y. Oh, A. I. Titov, and T.-S.-H. Lee, in *NSTAR 2000 Workshop: Excited Nucleons and Hadronic Structure*, edited by V. D. Burkert, L. Elouadrhiri, J. J. Kelly, and R. C. Münch, (World Scientific, Singapore, 2000), pp. 255-262, nucl-th/0004055.
- [21] N. I. Kochelev and V. Vento, *Phys. Lett. B* **515**, 375 (2001); **541**, 281 (2002).
- [22] A. Bramon, R. E. Scribano, J. L. Lucio M., and M. Napsuciale, *Phys. Lett. B* **517**, 345 (2001).
- [23] A. Gokalp and O. Yilmaz, *Phys. Lett. B* **508**, 345 (2001).
- [24] A. Donnachie and P. V. Landshoff, *Phys. Lett. B* **296**, 227 (1992).
- [25] P. G. O. Freund, *Phys. Lett. B* **2**, 136 (1962).
- [26] P. G. O. Freund, *Nuovo Cimento 5A*, **9** (1971).
- [27] R. Carlitz, M. B. Green, and A. Zee, *Phys. Rev. Lett.* **26**, 1515 (1971).
- [28] Yu. N. Kav and V. V. Serebryakov, *Nucl. Phys. B* **52**, 141 (1973).
- [29] A. Donnachie and P. V. Landshoff, *Nucl. Phys. B* **244**, 322 (1984).
- [30] P. V. Landshoff and O. Nachtmann, *Z. Phys. C* **35**, 405 (1987).
- [31] J.-M. Laget and R. Menendez-Galain, *Nucl. Phys. A* **581**, 397 (1995).
- [32] M. A. Pichowsky and T.-S.-H. Lee, *Phys. Rev. D* **56**, 1644 (1997).
- [33] A. I. Titov, Y. Oh, S. N. Yang, and T. Mori, *Phys. Rev. C* **58**, 2429 (1998).

[34] R. M. Achleidt, K. Holinde, and C. E. Ister, *Phys. Rep.* **149**, 1 (1987).

[35] A. Gokalp and O. Yilmaz, *Phys. Rev. D* **64**, 034012 (2001).

[36] T. M. Aliev, A. Ozpineci, and M. Savc, *Phys. Rev. D* **65**, 076004 (2002).

[37] SND Collaboration, M. N. Achasov et al., *Phys. Lett. B* **537**, 201 (2002).

[38] A. Bramon and R. Escribano, *hep-ph/0305043*.

[39] Particle Data Group, K. Hagiwara et al., *Phys. Rev. D* **66**, 010001 (2002).

[40] B. C. Pearce and B. K. Jennings, *Nucl. Phys. A* **528**, 655 (1991).

[41] T. Sato and T.-S. H. Lee, *Phys. Rev. C* **54**, 2660 (1996).

[42] H. Goldberg, *Phys. Rev.* **171**, 1485 (1968).

[43] H. Pilkuhn, W. Schmidt, A. D. Martin, C. Michael, F. Steiner, B. R. Martin, M. M. Nagels, and J. J. de Swart, *Nucl. Phys. B* **65**, 460 (1973).

[44] B. Renner, *Phys. Lett.* **33B**, 599 (1970).

[45] P. Aichuthan, H.-G. Schlaile, and F. Steiner, *Nucl. Phys. B* **24**, 398 (1970).

[46] J. Engels, *Nucl. Phys. B* **25**, 141 (1970).

[47] N. H. Egedgaard-Jensen, *Nucl. Phys. B* **119**, 27 (1977).

[48] E. Borie and F. Kaiser, *Nucl. Phys. B* **126**, 173 (1977).

[49] B. Renner, *Nucl. Phys. B* **30**, 634 (1971).

[50] M. Bando, T. Kugo, and K. Yamawaki, *Phys. Rep.* **164**, 217 (1988).

[51] J. Ballam et al., *Phys. Rev. D* **5**, 545 (1972).

[52] D. H. Sharp and W. G. Wagner, *Phys. Rev.* **131**, 2226 (1963).

[53] S. Weinberg, *Phys. Rev.* **133**, B1318 (1964).

[54] S.-J. Chang, *Phys. Rev.* **148**, 1259 (1966).

[55] S. Bellucci, J. Gasser, and M. E. Sainio, *Nucl. Phys. B* **423**, 80 (1994).

[56] D. Toublan, *Phys. Rev. D* **53**, 6602 (1996), **57**, 4495 (E) (1998).

[57] M. Suzuki, *Phys. Rev. D* **47**, 1043 (1993).

[58] K. Ramam, *Phys. Rev. D* **3**, 2900 (1971).

[59] H. Terazawa, *Phys. Lett. B* **246**, 503 (1990).